Spectroscopic measurements and terahertz imaging of the cornea using a rapid scanning terahertz time domain spectrometer*

Wen-Quan Liu(刘文权)[1,2,3,4], Yuan-Fu Lu(鲁远甫)[1,2,4,†], Guo-Hua Jiao(焦国华)[1,2,4], Xian-Feng Chen(陈险峰)[5], Zhi-Sheng Zhou(周志盛)[1,2,4], Rong-Bin She(佘荣斌)[1,2,4], Jin-Ying Li(李金瑛)[6], Si-Hai Chen(陈四海)[1,2,4], Yu-Ming Dong (董玉明)[1,2,4], and Jian-Cheng Lv(吕建成)[1,2,4]

[1] *Shenzhen Institutes of Advanced Technology, Chinese Academy of Sciences, Shenzhen* 518055, *China*
[2] *Biomedical Engineering Laboratory for Photoelectric Sensing Technology, Shenzhen* 518055, *China*
[3] *Shenzhen College of Advanced Technology, University of Chinese Academy of Sciences, Shenzhen* 518055, *China*
[4] *The Chinese University of Hong Kong, Shatin, Hong Kong, China*
[5] *School of Electronic Engineering, Bangor University, Bangor, Gwynedd LL57 1UT, UK*
[6] *Department of Ophthalmology, Peking University Shenzhen Hospital, Shenzhen* 518036, *China*

(Received 17 December 2015; revised manuscript received 22 March 2016; published online 25 May 2016)

Spectroscopic measurements and terahertz imaging of the cornea are carried out by using a rapid scanning terahertz time domain spectroscopy (THz-TDS) system. A voice coil motor stage based optical delay line (VCM-ODL) is developed to provide a rather simple and robust structure with both the high scanning speed and the large delay length. The developed system is used for THz spectroscopic measurements and imaging of the corneal tissue with different amounts of water content, and the measurement results show the consistence with the reported results, in which the measurement time using VCM-ODL is a factor of 360 shorter than the traditional motorized optical delay line (MDL). With reducing the water content a monotonic decrease of the complex permittivity of the cornea is observed. The two-term Debye relaxation model is employed to explain our experimental results, revealing that the fast relaxation time of a dehydrated cornea is much larger than that of a hydrated cornea and its dielectric behavior can be affected by the presence of the biological macromolecules. These results demonstrate that our THz spectrometer may be a promising candidate for tissue hydration sensing and practical application of THz technology.

Keywords: terahertz, rapid scanning terahertz time domain spectrometer, tissue diagnostics, terahertz imaging

PACS: 07.57.Pt, 78.20.Ci, 87.64.–t, 87.85.Pq **DOI:** 10.1088/1674-1056/25/6/060702

1. Introduction

Bound between microwaves and the infrared, the terahertz (THz) waves bridge the gap between electronics and optics and hold a wealth of intriguing and highly complex THz-matter interactions in physical, chemical and biological systems.[1] Recent research in THz medical imaging suggested that THz systems may be ideal for mapping the distribution and movement of water in physiologic tissues, especially in corneal tissues.[2,3] Over the last 3 decades, terahertz time-domain spectroscopy (THz-TDS) has emerged as a promising technique for numerous prospective studies, particularly for biomedical studies[4–10] as it gives direct access to the complex dielectric response of the bio-samples. Recent reports of the unique THz maps for the in vivo sensing of the corneal tissue[2,3] warrant further investigation into the THz properties of the cornea. To date, no experimental work on the dielectric properties of the cornea has been reported in the THz region, to our knowledge.[11,12]

It is important to know the THz dielectric properties of corneal tissue for understanding the interaction between THz radiation and cornea, from both fundamental and practical point of view. The drawback of conventional THz-TDS systems is the use of the motorized optical delay line (MDL) to realize the time delay between the THz pulse and the optical detection pulse. In particular, the traditional mechanical stage for time-delay scanning remains the bottleneck due to its reciprocating motion. It is difficult to introduce such a THz-TDS system into a high-speed performance. Hence, different high-speed systems have been proposed. For example, high-speed THz-TDS system based on asynchronous optical sampling (AOS) method was proposed as a promising method without any mechanical delay.[13–15] However, it is limited by the high cost of using two femtosecond (fs) lasers, the complex of phase lock system, and the dependence of temporal scan window on laser repetition rate. Various types of fast THz pulse measurements have been proposed, such as single-shot THz measurement, oscillating optical delay line, rotary optical delay line, rotation helicoid mirrors, circular involute stages, fiber stretcher, etc.[16–21] Hence, the simplest way to

*Project supported by the National Natural Science Foundation of China (Grant No. 61205101), the Shenzhen Municipal Research Foundation, China (Grant Nos. GJHZ201404171134305 and JCYJ20140417113130693), and the Marie Curie Actions-International Research Staff Exchange Scheme (IRSES) (Grant No. FP7 PIRSES-2013-612267).

†Corresponding author. E-mail: yf.lu@siat.ac.cn

© 2016 Chinese Physical Society and IOP Publishing Ltd

reduce time-delay scanning is to use a rapid scanning mechanical delay stage. The conventional MDL has a rather simple and robust structure, but in practice, it is not easy to provide a large delay range while the scanning speed is keeping sufficiently high. There is an inherent trade-off between the range and the speed. Voice coil motors (VCMs) are direct drive actuators in which a permanent magnet field and a coil winding are used to generate a force. The characteristics of the VCM include simple structure, high thrust density, rapid response and easy control,[22] hence the VCM may be the ideal actuator for low-cost, high-speed and long-range linear optical delay line. Since the first VCM based optical delay line (VCM-ODL) was presented for the measurement of picosecond (ps) laser pulses,[23] the first THz-TDS system with high dynamic range and fast measurement speed has been developed and commercialized in recent years.[24] However, the acquisition time of one pulse trace varies with the chosen delay range, since the swing speed of the voice coil is maintained to be constant. Consequently, the effective scanning speed of this system depends on the scan range of delay line and the dynamic range depends on the number of averaged time traces.

In this paper, we propose a rapid scanning terahertz time domain spectroscopy system based on a fast-scan optical delay line. This delay line powered by a VCM stage with high-speed and high-precision can provide a delay range over 130 ps, reaching the scanning rate of up to 50 Hz, which is independent of its scan range. Thanks to the VCM stage, the system drastically reduces the acquisition time and achieves a high dynamic range in conjunction with fast measurement speed. The developed THz-TDS is used to measure the liquid water and *ex-vivo* rabbit cornea in a range of 0.1 THz–0.5 THz. In addition, we also investigate the possible origins of the spectrum differences among the samples by fitting the parameters of the double Debye model to our experimental data. Moreover, a proof-of-principle study on THz imaging of the water loss in the cornea is also performed.

2. Experimental setup

Figure 1 illustrates the setup of a standard THz-TDS system with fast scanning. A mode-locked Ti:sapphire laser is employed as a pump source with a central wavelength of 800 nm, an average power of 800 mW, and pulse width < 100 fs, and a repetition rate of 80 MHz. THz pulses are generated and detected with low-temperature GaAs photoconductive switches, which require femtosecond laser excitation. The THz temporal waveform is scanned by varying the time delay between the pump beam and the probe beam. The MDL for the step-scan mode and the VCM-ODL for the fast-scan mode are used to compare the THz pulse signals measured by the two methods. The key component of our system is the VCM-ODL, in which the operation speed (up to 50 Hz) of VCM scanning stage allows the use of the lock-in technique.[25] Therefore, the THz signals can be measured with the readout of the lock-in amplifier signal values from the THz detector. In our experiments, we use the lock-in amplifier with suitable reference frequency of 38 kHz as well as time constants of 30 ms, 300 μs, 100 μs, and 30 μs for step 1 Hz, 10 Hz, and 50 Hz mode, respectively. The retro reflector in the VCM-ODL is kept to be in motion for continuous and linear forward-backward movement. Consquently, the optical path difference changes linearly. The exact delay time can be calculated from $2L/c$, where L is displacement of retro reflector and c is the speed of light. To drive VCM stage, a motion controller is installed to send the command from the computer to the stage and to provide a high-speed digitizer with the TTL signal as digital triggers. Then the data for the pulsed THz signal are recorded by the computer. Data acquisition is accomplished during the movement of the delay line. For the data acquisition process, control software is implemented in LabView^{TM}.

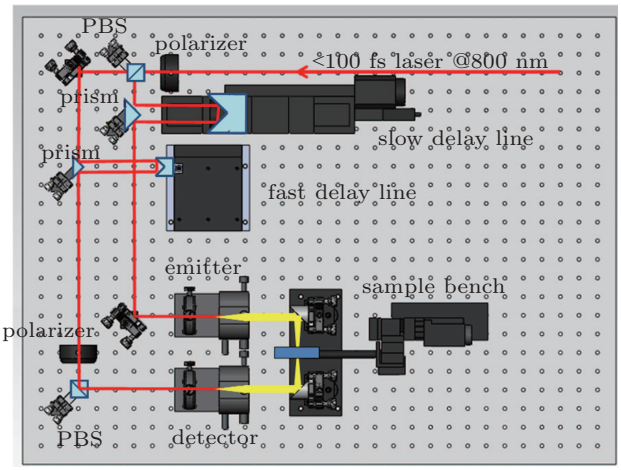


Fig. 1. (color online) Schematic representation of experimental setup for terahertz time domain system used to measure the properties of the cornea. PBS: prism beam splitter which separates laser pulsed into pump and probe beam.

3. System performance

VCM-ODL combines with a digital, high-precision position sensor with a resolution of 0.1 μm. Compared with the system (time resolution of 1.3 fs) described in Ref. [24], our system determines the delay position with an uncertainty below 200 nm, and thus achieves a higher time resolution of 0.67 fs. Meanwhile, such a delay line can provide a maximum continuous moving speed of 2 m/s with a stroke of 20 mm, corresponding to the highest scan rate of 100 Hz with the maximum delay range over 130 ps. Consequently, our system could reach the highest rate of 13000 ps/s, 10 times higher than that of 1200 ps/s (reported in Ref. [24]). Moreover, the scan rate of this delay line can vary with the chosen speed of the VCM stage, which does not depend on the delay range.

In order to examine the performance of our system, we carry out several independent tests in terms of THz spectral

amplitude at different scan rates under the same measurement environment. Figure 2 shows typical time-domain signals measured with our system using the fast delay line at 1 Hz, 10 Hz, and 50 Hz, respectively, where single traces of 35 ps are acquired in about 1 s, 95 ms, 15 ms at 1 Hz, 10 Hz, and 50 Hz mode, respectively. The width of the terahertz pulse, i.e. the time difference between the maximum and minimum amplitude, amounts to 870 fs. The system noise is also measured to determine whether the THz signal is reliable for analysis.

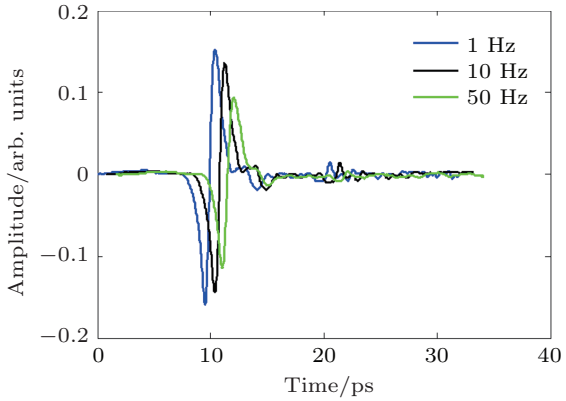


Fig. 2. (color online) Typical THz signal measured with our system with using the fast delay line at 1 Hz (blue curve), 10 Hz (black curve shifted +1 ps), and 50 Hz (green curve shifted +2 ps), respectively.

Figure 3 shows the representative spectra of the pulsed THz signals with chosen scanning speeds (step, 1 Hz, 10 Hz, and 50 Hz) respectively. Compared with data measured in step scan mode, it can be seen in Fig. 3(a) that the spectral amplitude of THz signal on logarithmic scale slightly decreases with scanning speed increasing while the noise floor increases. The corresponding noise floors in fast-scan modes (1 Hz, 10 Hz, and 50 Hz) are significantly higher than those in step-scan mode, which may be caused by the degradation of performance of suppressing the noise for lock-in amplifier which results from time constant decrease. The magnitudes of the noise floor increase with increasing scanning speed and they are about 0.0001, 0.0056, 0.0073, and 0.0099 at step, 1 Hz, 10 Hz, and 50 Hz mode, respectively. As a conservative estimation for fast-scan mode, the noise floor is set to be 0.0099, which implies that for the system the usable bandwidth above the measured noise floor is about 1.65 THz. To make spectral peaks rather readable, in Fig. 3(b) the spectral amplitudes of THz signal with chosen scanning speeds (step, 1 Hz, 10 Hz, and 50 Hz) are plotted on linear scale. There are slight differences among their spectral peak values (about 6.07, 5.90, 5.37, and 4.63 at step, 1 Hz, 10 Hz, and 50 Hz mode, respectively). Especially the spectra between the step and 1 Hz mode are remarkably similar. Consequently, its peak dynamic range (PDR) is at least 53 dB. The inset in Fig. 3(b) shows the dependence of the corresponding PDR on the scan rate of THz pulse. For the step mode measurement, the PDR is over 90 dB. This value decreases with the increase of scan rate: for 1 Hz mode and a total acquisition time of only 1 s, a PDR of 60 dB is obtained. The PDR decreases to 53 dB for 50 Hz mode. Therefore, our system can offer comparable THz spectroscopy at the scanning rate up to 50 Hz.

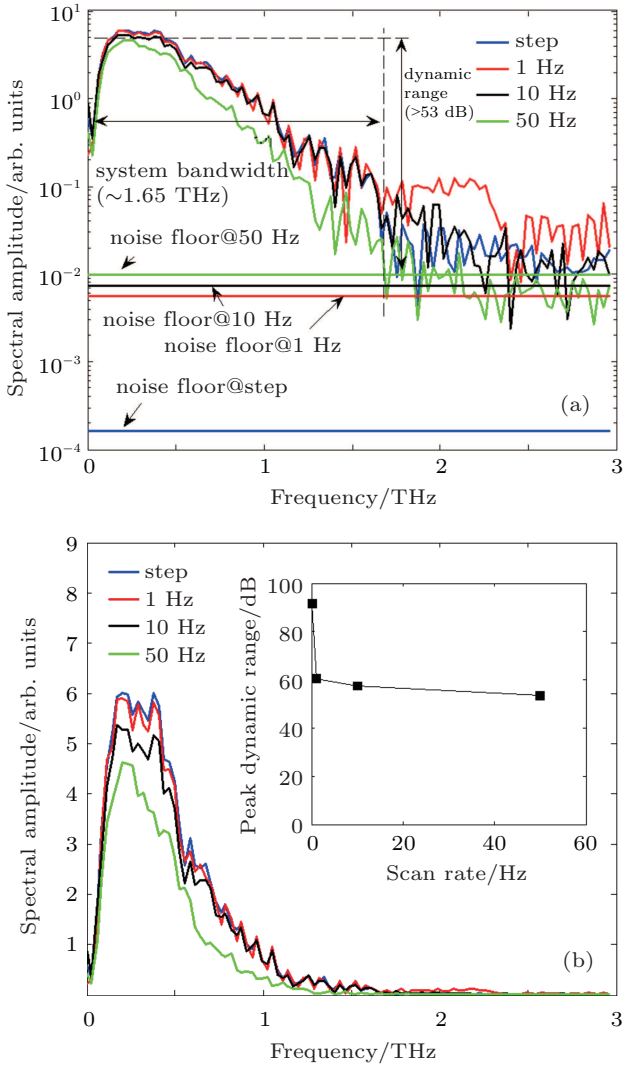


Fig. 3. (color online) Spectral amplitudes of pulsed THz signal on logarithmic (a) and linear (b) scale with chosen scanning speed, respectively. Step mode data: blue; 1 Hz mode data: red; 10 Hz mode data: black; 50 Hz mode data: green. The inset in Fig. 3(b) shows the dependence of the peak dynamic range (PDR) on the scan rate of THz pulse.

4. Results and discussion

Because THz radiation is strongly absorbed in water, it is ideal for determining the water content in corneal tissue. In this study, we measure THz spectrum at 1 Hz mode as the overlapping spectra with step-scan mode below 1.65 THz indicate the promising reliability in 1 Hz mode for rapid scanning THz-TDS. We perform the THz spectroscopic measurements of the cornea with different amounts of water content caused by different dehydration times.[26] The transmission spectra in a range of 0.1 THz–0.5 THz have been monitored to determine the refractive indexes and absorption coefficients of the water and the cornea. Figure 4 shows the refractive indices and absorption coefficients for distilled water and the

higher-hydrated cornea. The refractive indices monotonically decrease with increasing frequency, while the absorption coefficients monotonically increase with increasing frequency. No identifiable absorption lines are found in any of the spectra. The result for distilled water agrees very well with the published results,[27,28] while the values for hydrated cornea (especially absorption coefficient) are in close agreement with the simulation result reported by Taylor *et al.*[3] Although the tendency of the absorption coefficient of hydrated corneal tissue is similar to that of water, they are significantly different over most of the frequency range investigated. Both the refractive index and absorption coefficient of the cornea are smaller than those of distilled water.

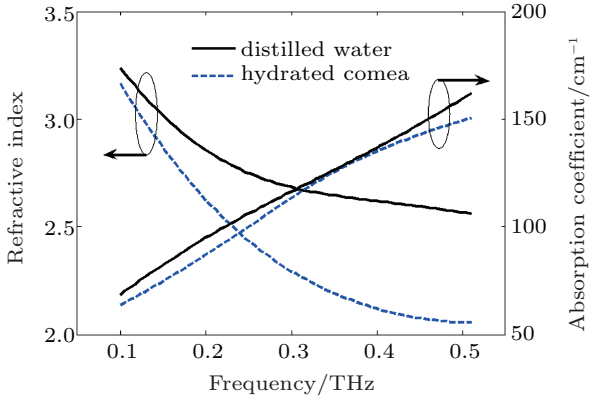


Fig. 4. (color online) Optical properties, refractive indexes, and absorption coefficients for distilled water (black solid line) and hydrated cornea (blue dashed line) versus THz frequency.

For describing the picosecond relaxation process in a material, e.g., in the water and corneal tissue, it is convenient to express the THz response in relative complex permittivity $\hat{\varepsilon}(\omega) = \hat{n}^2(\omega) = (n(\omega) - \mathrm{j}\kappa(\omega))^2 = \varepsilon'(\omega) - \mathrm{j}\varepsilon''(\omega)$. Here, $\kappa(\omega)$ is the extinction coefficient related to the absorption coefficient $\alpha(\omega)$ through $\kappa(\omega) = \alpha(\omega)c/(2\omega)\varepsilon'(\omega)$ and $\varepsilon''(\omega)$ are the real and imaginary part of the relative complex permittivity. For the sake of brevity, the term "relative" will henceforth be omitted. The complex dielectric coefficients in a range of 0.1 THz–0.5 THz are then calculated from the measured absorption coefficient and refractive indices for all the samples. Figure 5 shows the representative data of the measured dielectric properties for the corneal tissues in comparison with the distilled water with dehydration times of 24 h, 48 h, and 144 h, corresponding to higher-hydrated, lower-hydrated, and dehydrated cornea, respectively. In general, both the real and the imaginary parts of the permittivities for the water and the cornea nonlinearly decrease with frequency increasing, except for the dehydrated cornea (dehydration time of 144 h). With the water content (increasing dehydration time) decreasing, it can be seen that both the real and the imaginary part of the permittivity of the cornea monotonically decrease. Figure 5(a) shows that the real part of permittivity of water is greater than that of the cornea. It is clear that the real permittivity of the water decreases nonlinearly from 10.43 to 6.58 when the frequency increases from 0.1 THz to 0.5 THz. For the higher-hydrated cornea (dehydration time of 24 h), the real part of permittivity decreases from 9.92 to 4.19 with frequency increasing. The lower-hydrated cornea (dehydration time of 48 h) has the real part of permittivity, the magnitude of which decreases with increasing frequency and it varies in a range between 4.77 at 0.1 THz and 2.43 at 0.5 THz. For the dehydrated cornea (dehydration time of 144 h), it is approximately invariant in a range between 1.51 at 0.1 THz and 1.32 at 0.5 THz.

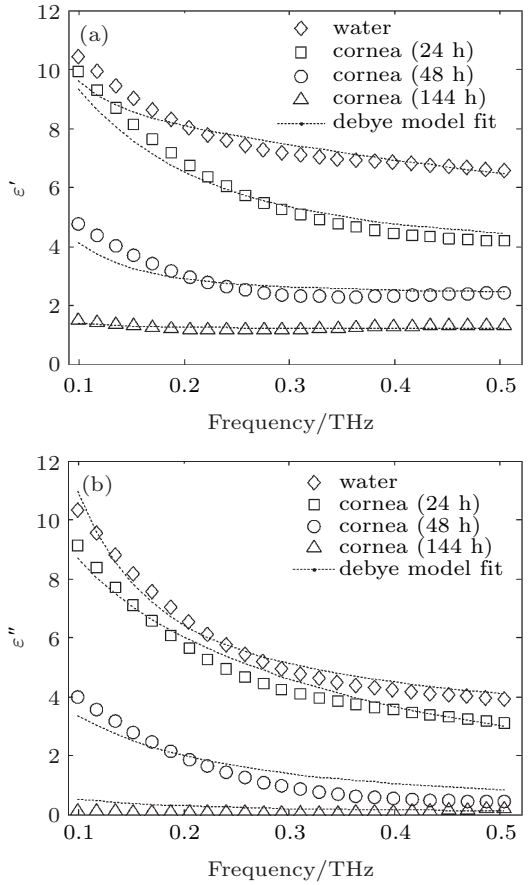


Fig. 5. (a) Real and (b) imaginary dielectric coefficients of distilled water and cornea with different amounts of water content caused by dehydration time. water data: diamonds; cornea (24 h) data: squares; cornea (48 h) data: circles; cornea (144 h) data: triangles; Debye model fit data: dashed lines.

Figure 5(b) shows that the plots are similar to experimental results for the imaginary parts of the permittivities of distilled water and the cornea. The water has the imaginary part of the permittivity which decreases from 10.31 to 3.93 with frequency increasing. The higher-hydrated cornea has the imaginary part of the permittivity which decreases with frequency increasing and its value varies from 9.12 at 0.1 THz to 3.11 at 0.5 THz. The imaginary part of the permittivity for lower-hydrated cornea is much smaller than the higher-hydrated one. Its value varies from 4.00 at 0.1 THz to 0.43 at 0.5 THz. For the dehydrated cornea, the imaginary part of the permittivity shows much flatter and decreases in a range between approximately 0.11 and 0.19. It is obvious that the permittivity spectra depend strongly on the hydration level in

the corneal tissue. Here, an effective model of the cornea system could be a mixture of water and biological background material (dehydrated cornea).[29] Since water is removed from the corneal tissue, it is logical that the permittivity should be reduced by the dehydrating process and becomes closer to that of background material.

The Debye theory describes the reorientation of molecules which could involve translational and rotational diffusion, hydrogen bond arrangement and structural rearrangement. The dielectric properties in the low THz frequency range of water have been characterized and well described by the double Debye model with a slow and a fast relaxation process.[30] Moreover, the Debye theory has been also used to understand the interaction of THz radiation with biological tissues.[28,31] To better understand the change in dielectric properties of the cornea with the dehydration, we employ the double Debye dielectric relaxation model given by

$$\hat{\varepsilon}(\omega) = \varepsilon_\infty + \frac{\varepsilon_s - \varepsilon_2}{1 + j\omega\tau_1} + \frac{\varepsilon_2 - \varepsilon_\infty}{1 + j\omega\tau_2}, \quad (1)$$

where ω is the angular THz frequency, ε_∞ is the dielectric constant in the high frequency limit (optical dielectric constant), ε_s is the static (zero frequency, DC) dielectric constant, ε_2 is the intermediate dielectric constant, τ_1 is the first Debye relaxation time, τ_2 is the second Debye relaxation time, and j $= \sqrt{-1}$. The differences $\varepsilon_s - \varepsilon_2$ and $\varepsilon_2 - \varepsilon_\infty$ are accordingly relative measures of the contributions of two relaxation processes to the macroscopic polarization.

Further, a genetic algorithm (GA) is chosen to fit the data to the Debye model by Eq. (1) because of its heuristic ability to quickly scan the vast solution. It is constrained by the initial population range for each of the Debye parameters. As can be seen from Fig. 5, the experimental dielectric properties for each sample could be described well by the double Debye function even though there are slight differences between the measured and simulated data below 0.15 THz. The fitted values of the parameters in the double Debye model fits to the measured data are summarized in Table 1.

Table 1. Double Debye coefficients for water and cornea.

	ε_∞	ε_s	ε_2	τ_1/ps	τ_2/ps
Water	3.99	74.01	9.99	8.06	0.26
Cornea (24 h)	3.84	45.01	9.98	9.14	0.99
Cornea (48 h)	2.38	20.02	9.56	59.97	2.85
Cornea (144 h)	1.20	7.48	2.19	68.97	3.10

In Table 1, ε_∞ is the dielectric constant in the high frequency limit (optical dielectric constant), ε_s the static (zero frequency, DC) dielectric constant, ε_2 the intermediate dielectric constant, τ_1 the first Debye relaxation time, and τ_2 the second Debye relaxation time.

Considering the data in Table 1, the fitted results for distilled water are in close agreement with previously reported results, and it is shown that the response of water in this frequency range can be described with two main Debye relaxation processes having relaxation times of ~8 ps and ~0.2 ps.[30] Moreover, for higher hydrated cornea (dehydration time of 24 h), the fitted results are consistent with microwave data.[11,32] The significant and important deduction to be made from Table 1 is that in all cases both the two relaxation times for the corneal tissues are generally much longer than the value for the distilled water. It is likely that the corneal dielectric behavior is affected by the biological macromolecules existing in the organic environment. When the cornea water content is higher, water molecules mainly affect the corneal dielectric function close to the water. However, the alteration in dielectric behavior could be caused by the proportion of the water tightly bound to neighboring macromolecules (water of hydration),[11] resulting in a restriction to the rotational ability of at least some of the tissue water molecules due to the organic environment.[32] The fast relaxation process is generally assigned to the relaxation from hydrogen bonding or relaxation of water molecules.[30,33] In this case it is difficult to promote the presence of individual molecules as the water. There could be much less dipoles participating in the fast relaxation as the water is removed from the corneal tissue, hence it is logical that two main Debye relaxation processes with relaxation times of the cornea are much longer than those of the water. Furthermore, the differences ($\varepsilon_s - \varepsilon_2$ and $\varepsilon_2 - \varepsilon_\infty$) for fast relaxation in the corneal tissues decrease significantly with reducing hydration level. This also indicates that there could be much less dipoles participating in the fast relaxation as the water content of the cornea decreases. A similar behavior has also been observed in ocular tissues to microwave data.[11,32]

Besides THz spectroscopy, we propose a THz image extension for our THz-TDS system. It moves the sample in the THz focal plane where a THz temporal waveform is recorded for each step of the XY-scanning stage. THz waves interacting with the cornea respond to the characteristics by changing their temporal behavior. Thus, this image of a cornea consists of $M \times N$ pixels, and is at one time instance along a discretized time domain with P points. By stacking these $M \times N$ arrays over time, a three-dimensional (3D) time domain array ($M \times N \times P$) is generated. With the fast Fourier transform (FFT) of the time domain data, THz spectral image of the cornea can be reconstructed. For proof-of-principle experiments, we monitor the loss of water from the cornea by using the THz spectral amplitude imaging of the ex-vivo rabbit cornea sample. In order to keep the sample flat and to avoid the geometry variations during the experiment, the cornea was placed in the sample cell during dehydration.[26] The cornea placed in the sample cell is dehydrated in drying oven for over

144 h to remove its water and the mass of the corneal tissue decreases as water loses. During the dehydration, we carry out the THz imaging measurement (Fig. 6(a)) at regular time intervals (i.e., 24 h). Each image is accompanied with its computed average water content in corneal tissue via using sample mass measurement. The average water concentration then can be calculated as $m_{\text{water}}/(m_{\text{water}} + m_{\text{drycornea}})$, where m_{water} and $m_{\text{drycornea}}$ are the mass of water in the cornea and the mass of water in the dry corneal tissue respectively.

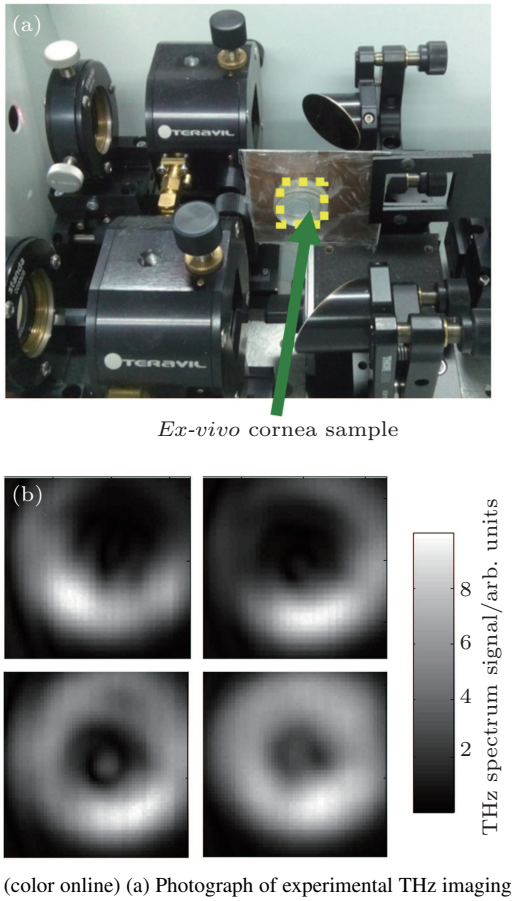


Fig. 6. (color online) (a) Photograph of experimental THz imaging setup. (b) THz spectral amplitude image (at 0.3 THz) of *ex-vivo* rabbit cornea at (upper-left to lower-right) 83%, 73%, 65%, and 41% average water content by mass.

The size of the scanned area is 21 mm × 21 mm and the step size is 0.5 mm. The THz spectrum for each pixel could be obtained by the rapid scanning THz-TDS technique at 1 Hz mode. The data acquisition time for one pixel is about 1.7 s for neighboring pixels in the same line, resulting in a total measurement time about 53 min. Figure 6 shows a photograph of THz imaging setup and THz spectral amplitude images of the *ex-vivo* cornea sample with different amounts of water content.

According to the performance of our system, the choice of THz imaging frequency is motivated by the trade-off among the image contrast, the spatial resolution and signal quality, which is observed to be well balanced at 0.3 THz. Figure 6(b) shows the corneal dehydrating THz spectral amplitude images at 0.3 THz, which clearly reveal changes in cornea water content distribution. The corneas with average water content values at 83%, 73%, 65%, and 41% by mass are represented by the similar circular-shaped area centered in the window, respectively. The cornea is fully hydrated in the initial test, and therefore appear the dark areas across the THz image. Clear preferential drying from the outer edges is then seen in each of the images. The lower the corneal hydration, the less the dark area is. It is likely to be due to the fact that the transmission through the dehydrated cornea (weaker absorption) is larger than a hydrated one (stronger absorption). Here, a model of the cornea system could be a binary mixture of water and biological background material (dehydrated cornea) according to the effective media theory.[34] Actually, the most dehydrated biological tissues are transparent in THz range while water is highly opaque in this band.[35] Since water is removed from the corneal tissue, the absorption is also reduced and becomes closer to that of background material. Furthermore, the progress of drying from the outside-inward is the expected result due to the faster diffusion in the lateral directions than in the thickness direction.[36] It is also consistent with the previous observation reported by Bennett *et al.*[37] These results suggest that THz imaging can be ideally suited to monitor the cornea by using water as the dominant contrast mechanism and may provide a new perspective of ophthalmologic diagnostic.

It is apparent that THz radiation is sensitive to variations of hydration bonding and water content, hence THz spectroscopy and imaging can be an excellent non-contact probe of water content in corneal tissue. Future research will attempt: i) to further quantify the relationship between THz properties (such as dielectric functions) and corneal hydration, in particular, corneal disease-related hydration; ii) to extend the frequency to higher region in order to ensure a precise determination of the fast relaxation time and better understanding of the mechanisms behind the relaxation processes; and iii) to develop a compact mobile and more cost-effective THz system in reflection geometry. It is expected that THz technique will become the clinically-viable technology to non-invasively assess the hydration changes of ocular diseases in vivo.

5. Conclusion and perspectives

In this work, a rapid scanning terahertz time domain spectroscopy system is successfully developed by using a fast-scan optical delay line based on the VCM stage. Measurements at the scanning rate in value up to 50 Hz demonstrate the capability of the VCM as the actuator for a fast delay line. Compared with by using MDL, the measurement time is shortened by a factor of 360 by using the ODL-VCM, which holds great potential as a cost-effective linear optical delay line in a rapid scanning THz-TDS system. THz spectroscopy is applied to liquid water with the great agreement with the reported results. Further, the real and imaginary parts of the dielectric

constants of the corneas with different amounts of water content in the lower THz region (0.1 THz to 0.5 THz) are measured, revealing that dehydrating the sample can reduce the dielectric coefficients of the samples. The two-term Debye relaxation model is used to describe the experimental results of the dielectric functions satisfactorily. Both two relaxation times for the corneal tissue are much longer than those of water sample, indicating that the biomolecules may have effects on the structure and properties of the cornea sample. Our results also demonstrate that the developed THz-TDS system can be an excellent tool for investigating the hydration in biological sample. Moreover, THz spectral imaging technique is successfully used to monitor the water loss of an ex-vivo cornea. The proposed and developed THz-TDS system demonstrate the advantages as a biomedical tool for non-contact sensing of tissue hydration, especially for cornea diagnostic in the field of ophthalmology.

References

[1] Jepsen P U, Cooke D G and Koch M 2011 *Laser Photon. Rev.* **5** 124
[2] Taylor Z D, Garritano J, Shijun S, Bajwa N, Bennett D B, Nowroozi B, Tewari P, Sayre J W, Hubschman J P, Deng S X, Brown E R and Grundfest W S 2015 *IEEE Trans. Terahertz Sci. Technol.* **5** 184
[3] Taylor Z D, Garritano J, Sung S, Bajwa N, Bennett D B, Nowroozi B, Tewari P, Sayre J, Hubschman J P, Deng S, Brown E R and Grundfest W S 2015 *IEEE Trans. Terahertz Sci. Technol.* **5** 170
[4] Castro-Camus E, Palomar M and Covarrubias A A 2013 *Sci. Rep.* **3** 2910
[5] Park S J, Hong J T, Choi S J, Kim H S, Park W K, Han S T, Park J Y, Lee S, Kim D S and Ahn Y H 2014 *Sci. Rep.* **4** 4988
[6] Oh S J, Kim S H, Jeong K, Park Y, Huh Y M, Son J H and Suh J S 2013 *Opt. Express* **21** 21299
[7] Dong C, Bao R M, Zhao K, Xu C H, Jin W J and Zhong S X 2014 *Chin. Phys. B* **23** 127802
[8] Jin W J, Li T, Zhao K and Zhao H 2013 *Chin. Phys. B* **22** 118701
[9] Zhou Q L, Shi Y L, Zhao D M, Zhang C L, Zhao S Q, Zhao H, Bao R M, Zhu S M, Miao Q, Tian L and Zhao K 2011 *Chin. Phys. B* **20** 010703
[10] Bennett D, Taylor Z D, Tewari P, Sung S, Maccabi A, Singh R, Culjat M, Grundfest W, Hubschman J P and Brown E 2012 *J. Biomed. Opt.* **17** 097008
[11] Gabriel C, Sheppard R J and Grant E H 1983 *Physics in Medicine and Biology* **28** 43
[12] Saviz M and Faraji-Dana R 2013 *Prog. Electromag. Res.* **137** 389
[13] Klatt G, Gebs R, Schäfer H, Nagel M, Janke C, Bartels A and Dekorsy T 2011 *IEEE Sel. Top. Quantum Electron.* **17** 159
[14] Yasui T, Saneyoshi E and Araki T 2005 *Appl. Phys. Lett.* **87** 061101
[15] Wilk R, Hochrein T, Koch M, Mei M and Holzwarth R 2011 *J. Opt. Soc. Am. B* **28** 592
[16] Yellampalle B, Kim K Y, Rodriguez G, Glownia J H and Taylor A J 2005 *Appl. Phys. Lett.* **87** 211109
[17] Jin Y S, Jeon S G, Kim G J, Kim J I and Shon C H 2007 *Rev. Sci. Instrum.* **78** 023101
[18] Kim G J, Jeon SG, Kim J I and Jin Y S 2008 *Rev. Sci. Instrum.* **79** 106102
[19] Molter D, Ellrich F, Weinland T, George S, Goiran M, Keilmann F, Beigang R and Léotin J 2010 *Opt. Express* **18** 26163
[20] Xu J Z and Zhang X C 2004 *Opt. Lett.* **29** 2082
[21] Gente R, Born N, Voβ N, Sannemann W, Léon J, Koch M and Castro-Camus E 2013 *J. Infrared Millim. Terahertz Waves* **34** 316
[22] Li L, Ma M, Bao B and Chen Q 2011 *IEEE Trans. Plasma Sci.* **39** 127
[23] Sala K L, Kenney-Wallace G A and Hall G E 1980 *IEEE J. Quantum Electron.* **QE-16** 990
[24] Vieweg N, Rettich F, Deninger A, Roehle H, Dietz R, Gobel T and Schell M 2014 *J. Infrared Milli. Terahz Waves* **35** 823
[25] Vieweg N, Krumbholz N, Hasek T, Wilk R, Bartels V, Keseberg C, Pethukhov V, Mikulics M, Wetenkamp L and Koch M 2007 *Proc. SPIE* **6616** 66163M
[26] Liu W Q, Lu Y F, Jiao G H, Chen X F, Li J Y, Chen S H, Dong Y M and Lv J C 2016 *Opt. Commum.* **359** 344
[27] Thrane L, Jacobsen R H, Jepsen P U and Keiding S R 1995 *Chem. Phys. Lett.* **240** 330
[28] Pickwell E, Cole B E, Fitzgerald A J, Wallace V P and Pepper M 2004 *Appl. Phys. Lett.* **84** 2190
[29] Bennett D B, Li W, Taylor Z D, Grundfest W S and Brown E R 2011 *IEEE Sensors Journal* **11** 1253
[30] Rønne C, Åtrand P O and Keiding S R 1999 *Phys. Rev. Lett.* **82** 2888
[31] Truong B C, Tuan H D, Kha H H and Nguyen H T 2013 *IEEE Trans. Biomed. Eng.* **60** 1528
[32] Gabriel S, Lau R W and Gabriel C 1996 *Physics in Medicine and Biology* **41** 2271
[33] Rønne C and Keiding S R 2002 *Journal of Molecular Liquids* **101** 199
[34] Federici J F 2012 *J. Infrared Millim. Terahertz Waves* **33** 97
[35] Xu J, Plaxco K W and Allen S J 2006 *J. Chem. Phys.* **124** 036101
[36] Holden B O, Mcnally J J and Egan P 1988 *Curr. Eye Res.* **7** 601
[37] Bennett D B, Taylor Z D, Tewari P, Singh R S, Culjat M O, Grundfest W S, Sassoon D J, Johnson R D, Hubschman J P and Brown E R 2011 *J. Biomed. Opt.* **16** 057003